Differentiation of gram-negative intermembrane phospholipid transporter function by intrinsic substrate preference

Ashutosh K. Rai[a], Katsuhiro Sawasato[b], Anastasiia Kozlova[b], Genevieve C. Sparagna[c], Mikhail Bogdanov[b], and Angela M. Mitchell[a,#]

[a] Department of Biology, Texas A&M University, College Station, Texas, USA

[b] Department of Biochemistry and Molecular Biology, McGovern Medical School at The University of Texas Health Science Center at Houston, Houston, Texas, USA

[c] Department of Medicine, Division of Cardiology, University of Colorado Anschutz Medical Campus, Aurora, Colorado, USA

Running title: Phospholipid transporter substrate preference

Address correspondence to Angela M. Mitchell, amitchell@bio.tamu.edu

Keywords: phospholipid trafficking, gram-negative envelope, outer membrane, lipid metabolism, cold sensitivity

Abstract: 250 words

Text: 5778 words

Abstract

The outer membrane of diderm Gram-negative bacteria acts as a barrier from chemical and physical stress. Anterograde phospholipid transport to the outer membrane has long been an area of intense investigation and, in *E. coli* K-12, it has recently been shown to be mediated by three related proteins: YhdP, TamB, and YdbH, which appear to provide hydrophobic channels for phospholipid diffusion, with YhdP and TamB playing the major roles. However, YhdP and TamB have different phenotypes suggesting distinct phospholipid transport functions. We investigated these functions using the synthetic cold sensitivity of a strain with Δ*yhdP* (but not Δ*tamB* or Δ*ydbH*) and Δ*fadR*, a transcriptional regulator allowing switching between fatty acid degradation and synthesis and regulating unsaturated fatty acid production. Deletion of *tamB*, forcing phospholipid transport to YdbH, suppresses the Δ*yhdP* Δ*fadR* cold sensitivity suggesting this phenotype is due to TamB dysfunction. Increased levels of cardiolipin and fatty acid saturation are necessary for cold sensitivity and lowering levels of either suppresses this sensitivity. Our data support a model where YhdP primarily transports more saturated phospholipids, TamB primarily transports phospholipids with more than one carbon unsaturation, and cardiolipin obstructs TamB by selectively clogging its channel. Thus, the multiple phospholipid transporters may allow the saturation state of the outer membrane to be regulated independently of the inner membrane by altering the YhdP-TamB activity ratio. Maintaining membrane physical integrity and function under changing conditions may require envelope remodeling including altered phospholipid composition and intermembrane trafficking. Our data provide a potential mechanism for this regulation.

50 **Importance**

51 Gram-negative bacteria possess an impermeable outer membrane protecting against
52 environmental stress and antibiotics. Outer membrane phospholipid transport remained
53 mysterious until recently when YhdP, TamB, and YdbH were implicated in phospholipid
54 transport between the inner and outer membranes of *E. coli*. TamB also modulates
55 phospholipid transport in a distantly related diderm Fermicute. Here, we investigate
56 functional differentiation between YhdP and TamB. Our data strongly suggest YhdP's and
57 TamB's functions are distinguished by the saturation state of phospholipids with YhdP
58 preferentially transporting more saturated phospholipids and TamB transporting more
59 unsaturated phospholipids. Cardiolipin headgroup specificity may also contribute to
60 TamB inhibition, perhaps due to the bulky nature of cardiolipin inhibiting the passage of
61 other phospholipids. Diversification of function between YhdP and TamB provides a
62 mechanism for regulation of phospholipid composition, and possibly the mechanical
63 strength and permeability of the outer membrane, and so the cell's intrinsic antibiotic
64 resistance, in changing environmental conditions.

65

Introduction

The gram-negative bacterial cell envelope has an outer membrane (OM) that sits outside the aqueous periplasm and peptidoglycan cell wall. The OM provides a barrier against various environmental stresses including toxic molecules such as antibiotics and osmotic pressure (1-6). Unlike the inner membrane (IM), a phospholipid bilayer, the OM is largely composed of phospholipids (mainly phosphatidylethanolamine (PE) (7)) in its inner leaflet and LPS (lipopolysaccharide) in its outer leaflet (2, 8). However, both membranes are asymmetric as the IM has different phospholipid compositions in its inner versus outer leaflets (9). Outer membrane proteins (OMPs) form a network across the cell surface interspersed with phase separated LPS patches (10). Lipoproteins are generally anchored in the inner leaflet of the OM (11).

OM components are synthesized in the cytoplasm or IM and transported to the OM. OMP (12), lipoprotein (11), and LPS (13) transport pathways are well defined. However, until recently, intermembrane phospholipid transport (between the IM and OM), especially anterograde transport from the IM to the OM, has remained largely very poorly understood. Phospholipids are synthesized at the IM's inner leaflet (14) and rapid, bidirectional intermembrane phospholipid transport occurs (15), even without ATP (16). Phospholipid transport has a relaxed specificity, allowing transport of non-native lipids (17, 18); however, intermembrane phospholipid composition differences are maintained (7, 19-22). Establishment and maintenance of this defined lipid topography between the IM and the OM must involve the coordinated biosynthesis and balanced bidirectional trafficking of specific phospholipids across the IM and from the IM to the OM (23).

A recent study has demonstrated that anterograde phospholipid transport is mediated by a high-flux, diffusive system in *Escherichia coli* (24). The Mla system removes mislocalized phospholipids from the OM outer leaflet and returns them to the IM (25). A gain-of-function allele, *mlaA** (26, 27), opens a channel allowing phospholipids to mislocalize to the cell surface by flowing from the OM's inner to outer leaflet (26, 28), resulting in a PldA-mediated attempt to reestablish OM asymmetry by increasing LPS production, OM vesiculation, and increased flow of phospholipids to the OM (26, 27). When nutrients are depleted, inhibiting phospholipid production, cells lyse due to loss of IM integrity (16, 18). Single cell imaging of *mlaA** cells confirmed an aberrant lipid flow from the IM to the OM at a fast rate. Loss of YhdP, an inner membrane protein, could significantly slow phospholipid flow to the OM resulting in loss of OM integrity before IM rupture (24), suggesting YhdP might play a role in intermembrane phospholipid transport.

Very recently, YhdP and two homologs, TamB and YdbH, were demonstrated to be intermembrane phospholipid transporters (29, 30). Ruiz, *et al*. investigated AsmA family proteins and found Δ*yhdP* Δ*tamB* mutants showed synthetic OM permeability and stationary phase lysis (29). Moreover, when combined, Δ*yhdP*, Δ*tamB*, and Δ*ydbH* are synthetically lethal. Genetic interactions of these mutants with *mlaA* and *pldA* show their

105 involvement in OM phospholipid homeostasis. Predicted structures of YhdP, TamB, and
106 YdbH (31, 32), as well as a partial crystal structure of TamB (33), have a β-taco fold domain
107 with a hydrophobic pocket, resembling eukaryotic lipid transporters (34-37). These
108 structural findings are another clue that suggests YhdP, TamB, and YdbH are involved in
109 phospholipid transport. Douglass, *et al.* confirmed the synthetic lethality of Δ*yhdP*,
110 Δ*tamB*, and Δ*ydbH* and demonstrated a Δ*tamB* Δ*ydbH* mutant with reduced *yhdP*
111 expression had decreased amounts of OM phospholipids, directly demonstrating their
112 involvement in intermembrane phospholipid transport or its regulation (30), although *in*
113 *vitro* interaction of YhdP, TamB, and YdbH with phospholipids has yet to be investigated.
114 Nevertheless, the role of these proteins in phospholipid transport may be widely
115 conserved as recent evidence suggests TamB plays a role in anterograde phospholipid
116 transport in *Veillonella parvula*, a diderm Fermicute (38).

117 Nevertheless, why there are three separate intermembrane phospholipid transport
118 proteins and the functional interactions between these proteins remains unanswered,
119 although it is clear the proteins are not fully redundant or functionally equivalent. The
120 conditional expression of *yhdP* alone, without the presence of *ydbH* and *tamB*, fully
121 complements neither growth phenotypes nor a normal level of OM phospholipids,
122 suggesting transport function is still impaired in this strain (30). In addition, YdbH seems
123 to play a more minor role than YhdP and TamB (29, 30) and the screen identifying Δ*yhdP*
124 as slowing *mlaA**-dependent lysis did not identify Δ*tamB* or Δ*ydbH* (24). Moreover, we
125 previously identified a role for YhdP in stationary phase SDS (sodium dodecyl sulfate)
126 resistance and modulating cyclic enterobacterial common antigen activity (39, 40) not
127 shared by TamB and YdbH (**Fig. S1**) (29, 30, 39, 40).

128 Here, we investigated the differentiation of YhdP and TamB function and identified
129 synthetic cold sensitivity due to impaired TamB function in a strain with Δ*yhdP* and Δ*fadR*,
130 a transcriptional regulator of fatty acid biosynthesis and degradation, acting as a
131 transcriptional switch between these pathways in response to acyl-CoA (41). FadR is
132 necessary for normal levels of unsaturated fatty acids to be synthesized (42). We found
133 for the first time that the Δ*yhdP* Δ*fadR* mutant has increased levels of a specific
134 phospholipid, cardiolipin (CL), and decreasing CL suppresses cold sensitivity. Furthermore,
135 increasing unsaturated fatty acid levels suppresses cold sensitivity. Overall, our data lead
136 us to a model where TamB and YhdP functions are differentiated based on phospholipid
137 fatty acid saturation state, with TamB transporting more unsaturated phospholipids and
138 YhdP transporting more saturated phospholipids. Phospholipid species or head group can
139 also contribute to transport specificity, since higher levels of dianionic CL are necessary

140 for the cold sensitivity phenotype, potentially due to functional inhibition of TamB by
141 clogging of its hydrophobic groove.
142
143
144 **Results**

145 **Loss of FadR and YhdP results in cold sensitivity due to impaired TamB function.** To
146 investigate YhdP-TamB function differentiation, we created a Δ*yhdP* Δ*fadR* strain, as FadR
147 is a major regulator of lipid homeostasis (41). A deletion strain of *fadR* alone is expected
148 to have decreased fatty acid synthesis, increased fatty acid degradation, and increased
149 fatty acid saturation (41, 42). Surprisingly, Δ*yhdP* Δ*fadR* cultures grown at 30 °C lagged for
150 more than 8 hours, followed by highly variable growth, suggesting suppressor outgrowth
151 (**Fig.1A**). The growth defect was decreased at 37 °C and completely absent at 42 °C. To
152 confirm this cold sensitivity, we estimated efficiency of plating(EOP) and confirmed the
153 severe cold intolerance of the Δ*yhdP* Δ*fadR* strain (5 logs at 30 °C and 3 logs at 37 °C) (**Fig.
154 1B**). Although, cyclic enterobacterial common antigen is necessary for Δ*yhdP*'s OM
155 permeability phenotypes (40), the Δ*yhdP* Δ*fadR* strain's cold sensitivity was unchanged
156 when enterobacterial common antigen was not present (Δ*wecA*) (43) (**Fig. 1C**).

157 Given their involvement in phospholipid transport, we expected Δ*tamB* and/or Δ*ydbH* to
158 show similar synthetic phenotypes with Δ*fadR*; however, Δ*fadR* Δ*tamB* and Δ*fadR* Δ*ydbH*
159 strains had no growth defects (**Fig 1D**). We, therefore, hypothesized the Δ*yhdP* Δ*fadR* cold
160 sensitivity was due to impairment of another phospholipid transporter(s). Although
161 Δ*ydbH* in the Δ*yhdP* Δ*fadR* strain did not alter cold sensitivity (**Fig. 1E**), Δ*tamB* in the Δ*yhdP*
162 Δ*fadR* background completely suppressed the cold sensitivity (**Fig. 1F**). Consistent with
163 previous observations (29), the Δ*yhdP* Δ*fadR* Δ*tamB* strain was mucoid due to Rcs stress
164 response activation and colanic acid capsule production. Deleting *rcsB*, an Rcs response
165 regulator, prevented mucoidy but did not affect suppression (**Fig. 1F**). We observed only
166 minimal growth phenotypes in the Δ*yhdP* Δ*fadR* Δ*tamB* strain, similar to those of Δ*tamB*
167 and less severe than those of Δ*fadR* (**Fig. 1G**), eliminating slow growth as a suppression
168 mechanism. Together, these data demonstrate suppression from loss of TamB is due to
169 reprieve of impaired TamB function, shifting phospholipid transport to YdbH.

170 We next looked for envelope homeostasis alterations in the Δ*yhdP* Δ*fadR* strain with
171 TamB impairment. To identify cell lysis and/or severe OM permeability defects at 30 °C,
172 we assayed CPRG (chlorophenol red-β-D-galactopyranoside) processing. CPRG must
173 contact LacZ in the cytoplasm or supernatant to release chlorophenol red (44). Compared
174 to wild type or single mutants, the Δ*yhdP* Δ*fadR* strain had increased CPRG processing
175 (**Fig. S2A**), demonstrating lysis or increased envelope permeability. When we assayed
176 resistance to molecules excluded by the OM (1, 39, 40, 45, 46) at 37 °C, a semi-permissive
177 temperature, the Δ*yhdP* Δ*fadR* strain showed sensitivity to vancomycin, a large scaffold
178 antibiotic, and SDS EDTA compared to single mutants (**Fig. S2B**). However, with bacitracin
179 treatment or EDTA treatment alone, the Δ*yhdP* Δ*fadR* strain phenocopied the Δ*fadR*

single deletion (**Fig. S2CD**). LPS levels were not altered in the Δ*yhdP*, Δ*fadR*, or the Δ*yhdP* Δ*fadR* strain (**Fig. S2E**). OM asymmetry mutations (i.e., Δ*pldA*, Δ*mlaA*) (25-27, 47) did not have suppressive or synthetic effects on cold sensitivity in the Δ*yhdP* Δ*fadR* strain (**Fig. S3AB**), suggesting against a causal loss of OM asymmetry. Overall, the changes in OM permeability did not seem sufficient to cause lethality at lower temperature, suggesting the phospholipid transport disruption affects both IM and OM integrity.

Increased cardiolipin is necessary for impaired TamB function. We investigated phospholipid composition of the wild-type and Δ*yhdP* Δ*fadR* strains grown at the permissive temperature (42 °C) and grown to early log phase at 42 °C, then downshifted to 30 °C. *E. coli* phospholipid composition is generally 75% phosphatidylethanolamine (PE), 20% phosphatidylglycerol (PG), and 5% cardiolipin (CL) with CL increasing in stationary phase (14, 48). Of the three CL synthases, ClsA and ClsB synthesizes CL from two PG molecules, while ClsC synthesizes CL from one PG and one PE molecule, so CL and PG levels are generally reciprocally regulated(49-52). For both strains and conditions, the levels of PE were similar (**Fig. 2A**). However, the Δ*yhdP* Δ*fadR* strain had increased CL and concomitant decreased PG compared to the wild-type strain, especially at 30 °C. PgsA synthesizes phosphatidylglycerol-phosphate and is the first enzyme differentiating PG and PE biosynthesis. PgsA depletion would decrease both PG and CL levels, reversing increased CL levels and exacerbating decreased PG levels in the Δ*yhdP* Δ*fadR* strain. We tested the effect of PgsA depletion in a strain background (Δ*rcsF* Δ*lpp*) where *pgsA* is non-essential (53-56). When *pgsA* expression was induced (arabinose panel), the Δ*yhdP* Δ*fadR* PgsA-depletion strain had equal cold sensitivity to the Δ*yhdP* Δ*fadR* strain (**Fig. 2B**). When *pgsA* expression was repressed (glucose panel), the Δ*yhdP* Δ*fadR* cold sensitivity was partial suppressed, demonstrating that decreased PG does not cause for cold sensitivity and suggesting increased CL may be necessary for cold sensitivity. Indeed, the cold sensitivity of the Δ*yhdP* Δ*fadR* strain was lost when CL was fully depleted due to deletion of the genes for all cardiolipin syntheses (Δ*clsABC*) or of the gene for the main exponential phase cardiolipin synthase (Δ*clsA*) (**Fig. 2ACD**). Δ*clsB or* Δ*clsC* caused a smaller decrease in CL levels that was very similar between the two strains (11% to 7.4% vs. 7.6%, respectively) (**Fig. 2A**). Surprisingly, Δ*clsC* completely suppressed the cold sensitivity, while Δ*clsB* did not (**Fig. 2EF**). Thus, increased CL is necessary for impaired TamB function leading to cold sensitivity but CL levels alone cannot explain the phenotype: another factor, such as a specific molecular form (e.g., acyl chain length, saturation state, symmetry of acyl chain arrangement) or localization (e.g., poles vs. midcell or inner vs. outer leaflet)of CL, is required.

Increased *fabA* expression suppresses cold sensitivity. To identify other factors involved in the cold sensitivity, we applied a forward genetic approach by isolating spontaneous suppressor mutants capable of growing at 30 °C and identified a suppressor mutant (Suppressor 1) that restored growth at 30 °C (**Fig. 3A**), decreased CPRG processing (**Fig. S2A**), and had very similar CL to the Δ*yhdP* Δ*fadR* strain (**Fig. 3B**, **Fig. S4**). We identified a point mutation in the *fabA* promoter region in Suppressor 1 (**Fig. 3C**) and confirmed this

221 mutation was sufficient for suppression (**Fig. 3D**). FabA is a dehydratase/isomerase that
222 introduces *cis* unsaturation into fatty acids (14, 57) and *fabA* is expressed from two
223 promoters controlled by FadR and FabR (58, 59). FadR activates *fabA* expression, while
224 FabR represses. Thus, *fadR* deletion would be expected to lower *fabA* expression. The
225 suppressor mutation was located in the *fabA* promoter FabR binding site (**Fig. 3C**) and we
226 hypothesized this mutation would increase *fabA* expression. *fabA* mRNA levels were more
227 than 4-fold lower in the Δ*yhdP* Δ*fadR* strain than the wild-type strain (**Fig. 3E**). While lower
228 than wild type, the suppressor mutant increased *fabA* mRNA 1.6-fold over the Δ*yhdP*
229 Δ*fadR* strain.

230 We constructed luciferase reporter plasmids with the wild-type *fabA* promoter region or
231 the *fabA* promoter region containing the suppressor mutation. The reporter with the
232 mutated promoter had higher activity in a wild-type, Δ*fadR,* and Δ*fabR* background (**Fig.**
233 **3F**). *fabA* transcription occurs from a promoter downstream of the FabR binding site (59-
234 61). However, when *fadR* is deleted, transcription shifts to the FabR-regulated promoter
235 within the FabR binding region (59-61). Our data indicate the Suppressor 1 mutation
236 regulates this promoter's constitutive activity rather than FabR binding. To confirm the
237 effect of changing the second promoter's activity, we tested the effect of Δ*fabR* on cold
238 sensitivity in the Δ*yhdP* Δ*fadR* strain and observed partial suppression (**Fig. S5**). The
239 smaller effect of Δ*fabR* compared to Suppressor 1 may result from other gene expression
240 changes or to the smaller relative effect of Δ*fabR* on *fabA* expression (**Fig. 3F**). Overall,
241 these data demonstrate increasing *fabA* expression, which is necessary for unsaturated
242 fatty acid biosynthesis, rescue TamB's functional deficiency in the Δ*yhdP* Δ*fadR* strain
243 without changing CL levels.

244 **Increasing unsaturated fatty acids relieves impaired TamB function.** Given the effect of
245 *fabA* expression on the Δ*yhdP* Δ*fadR* cold sensitivity, we used liquid chromatography-
246 electrospray ionization mass spectrometry (LC/MS) to characterize the strains'
247 phospholipid saturation state (**Dataset S1**, **Fig. 4A-C, Fig. S6**). We analyzed whole cell and
248 IM extracts (**Fig. S6A**) from cells grown to early log phase at 42 °C then downshifted to 30
249 °C. As expected, in whole cell extracts, Δ*fadR* caused increased fully saturated and
250 monounsaturated PE with a concomitant decrease of diunsaturated PE (**Fig. 4A**, **Fig. S6B**).
251 Levels of fully saturated PG were also increased with a decrease in mono- and
252 diunsaturated species (**Fig. 4B**, **Fig. S6C**). Similarly, the Δ*fadR* strain demonstrated
253 increased monounsaturated CL with a concomitant decrease in triunsaturated CL (**Fig. 4C**,
254 **Fig. S6D**). Compared to the Δ*fadR* strain, the Δ*yhdP* Δ*fadR* strain had slightly increased
255 saturation for all three phospholipids, with the largest increase in fully saturated PE.
256 Suppressor 1 demonstrated decreased saturation of all three phospholipids but especially
257 of PE compared to the Δ*yhdP* Δ*fadR* strain (**Fig. 4A-C**, **Fig. S6E-G**). The OM is enriched for
258 PE and its saturated species compared to the IM outer leaflet (7, 9, 20-22) making the
259 large PE changes intriguing. We wondered whether the suppression difference between
260 Δ*clsC* and Δ*clsB* resulted from the CL saturation state. However, the Δ*yhdP* Δ*fadR* Δ*clsB*
261 and Δ*yhdP* Δ*fadR* Δ*clsC* strains had very similar CL profiles (**Fig. 4C**, **Fig. S6G**), suggesting

262 another qualitative difference affecting suppression, perhaps CL lateral or inter-leaflet
263 distribution in the cell.

264 We hypothesized increasing unsaturated fatty acids suppresses Δ*yhdP* Δ*fadR* cold
265 sensitivity and performed EOPs for cold sensitivity on media containing an unsaturated
266 fatty acid (oleic acid, C18:1 *cis*-9). Exogenous phospholipids can be taken up by *E. coli*,
267 attached to acyl-CoA, and incorporated into phospholipids (62). Oleic acid addition
268 suppressed the Δ*yhdP* Δ*fadR* strain's cold sensitivity (**Fig. 4D**). Supplementing oleic acid
269 increases unsaturated phospholipids and provides an exogenous fatty acid source. To
270 differentiate between saturation state and fatty acid availability, we compared treatment
271 with oleic acid and saturated stearic acid (C18:0). Only oleic acid, and not stearic acid,
272 suppressed the Δ*yhdP* Δ*fadR* strain's cold sensitivity (**Fig. 4E**), confirming increasing
273 unsaturated fatty acids, not fatty acid availability suppresses.

274 These data suggested the Δ*yhdP* Δ*fadR* strain was impaired in intermembrane transport
275 of more saturated phospholipids. To investigate phospholipid transport defects, we
276 compared phospholipids extracted from whole cells and isolated pure IM (**Fig. S6A**). We
277 did not use OM extracts as they are generally contaminated with IM, complicating
278 interpretation. PG and CL showed small differences between whole cell and IM extracts
279 but were largely similar between strains (**Fig. 4BC**). However, PE showed larger strain
280 differences. In the wild-type strain, fully saturated PE was enriched in whole cells
281 compared to IM, demonstrating OM enrichment of saturated PE (**Fig. 4A**, **Fig. S6H**). In
282 the Δ*fadR* strain, whole cell and IM extracts had similar fully saturated PE levels, but IM
283 extracts had higher amounts of diunsaturated PE, still suggesting disproportional OM
284 enrichment with more saturated PE. However, in the Δ*yhdP* Δ*fadR* strain, while the IM
285 had higher levels of diunsaturated PE, the IM was underrepresented for fully saturated
286 PE (**Fig. 4A**, **Fig. S6H**). The Δ*yhdP* Δ*fadR* IM also had much lower levels of short chain PE
287 (30:0 and 30:1) than whole cells (**Fig. 4A**, **Fig. S6HI**). Short chain phospholipids decrease
288 membrane rigidity and remain fluid at lower temperatures (63). Thus, the short fatty acid
289 PE increase after short-term adaptation to 30 °C may be a cellular attempt to increase
290 fluidity and restore homeostatic balance between the membranes. In Suppressor 1, the
291 profile more closely resembled Δ*fadR* cells. Thus, the alteration of PE saturation and fatty
292 acid length in the Δ*yhdP* Δ*fadR* OM demonstrates a disportortional distribution of
293 saturated and unsaturated PE as a consequence of disruption in intermembrane
294 phospholipid trafficking due to impairment of TamB function.

295 **Suppression causes fatty acid metabolism and stress response alterations.** In wild-type
296 cells, *fabA* overexpression does not change phospholipid saturation levels, demonstrating
297 the FabB enzyme is rate limiting for unsaturated fatty acid biosynthesis (64). We were
298 intrigued that Suppressor 1 altered saturation without directly effecting *fabB* expression.
299 We also wondered whether CL levels in the Δ*yhdP* Δ*fadR* strain are transcriptionally
300 regulated. Thus, we investigated the transcriptional landscape of the wild type, the Δ*yhdP*
301 Δ*fadR*, and Suppressor 1 strains after a 30 minute downshift of growth to 30 °C to

302 determine: (i) whether the Δ*yhdP* Δ*fadR* strain had altered *cls* gene expression; (ii)
303 whether Suppressor 1 had other transcriptional changes; and (iii) why increased *fabA*
304 expression decreased saturation. All differentially expressed genes (>2-fold change,
305 $p<0.05$) are listed in **Dataset S2**. Principle component analysis of these genes showed the
306 closest relation between Δ*yhdP* Δ*fadR* strain and Suppressor 1, while the wild-type strain
307 was more distantly related (**Fig. 5A**, **S7A**). Nevertheless, Suppressor 1 was more closely
308 related to wild type than was the Δ*yhdP* Δ*fadR* strain. Most differentially regulated genes
309 between Δ*yhdP* Δ*fadR* and wild type and Suppressor 1 and wild type were upregulated
310 (**Fig. 5BC**, **S7BC**). Many of the most highly regulated genes are FadR-regulon members.
311 The majority of differentially regulated genes in Suppressor 1 compared to Δ*yhdP* Δ*fadR*
312 are downregulated (**Fig. 5D, S7D**). These genes are involved in many cellular pathways
313 and likely reflect the decreased cellular stress (**Table S2**). Indeed, many external stress
314 response genes are more enriched in Δ*yhdP* Δ*fadR* than in Suppressor 1 (**Fig. S8A**).

315 No significant expression changes occurred in the CL biosynthesis pathway (**Fig. 5E**) or
316 other phospholipid biosynthesis genes (**Fig. S8B**). The increased cardiolipin in Δ*yhdP*
317 Δ*fadR* and Suppressor 1 may be post-transcriptional or due to a change in a regulatory
318 pathway not yet altered after 30 minutes at 30 °C (**Fig. S8C**). Levels of mitochondrial CL
319 can be altered due to differences in substrate binding affinity of the CL synthase based on
320 saturation, with increased saturation decreasing CL synthesis (65), and it may be that a
321 similar pathway operates here, albeit in a different direction. We examined the
322 expression of genes in fatty acid synthesis and degradation, many of which are members
323 of the FadR regulon. In Δ*yhdP* Δ*fadR* compared to wild type, many fatty acid biosynthesis
324 genes significantly decreased while many fatty acid degradation genes significantly
325 increased (**Fig. 5F**), consistent with Δ*fadR* effects. While *fabA* expression is decreased,
326 *fabB* expression is not changed, explaining why increased *fabA* expression causes
327 decreased saturation in Suppressor 1. Overall, our data demonstrate the Δ*yhdP* Δ*fadR*
328 strain's cold sensitivity is due to impaired TamB function, and increased phospholipid
329 saturation and cardiolipin are necessary for this functional impairment.

330

331

332 **Discussion**

333 The identification of YhdP, TamB, and YdbH as putative intermembrane phospholipid
334 transporters (29, 30) posed the tantalizing question: why is having three transporters
335 advantageous? Here, we demonstrate each protein plays a distinguishable role in
336 phospholipid transport that can be differentiated based on genetic interactions with lipid
337 metabolism. Disruption of FadR and YhdP function causes synthetic cold sensitivity not
338 shared by TamB or YdbH, due to impaired TamB function, which can be suppressed by
339 switching transport to YdbH. This phenotype requires both increased levels of CL and
340 saturated fatty acids, and decreasing amounts of either suppresses. In addition, our data
341 demonstrate CL synthesized by ClsB and ClsC is qualitatively different—resulting in
342 differential suppression phenotypes—likely due to differences in CL localization, CL-

343 mediated, leaflet-specific changes in lipid packing order (9, 23), localized membrane
344 fluidity (66), or TamB interaction.

345 In our model based on these data (**Fig. 6A-C**), the functions of YhdP and TamB are
346 diversified based on the acyl carbon saturation level preference of the phospholipids they
347 transport: YhdP transports mainly phospholipids with more saturated fatty acids, while
348 TamB transports phospholipids with more unsaturated fatty acids (**Fig. 6A**). Our data and
349 previous data (29, 30) agree YdbH plays a relatively minor role. In the Δ*yhdP* Δ*fadR* strain,
350 YhdP's absence forces more saturated phospholipids to be transported by TamB. At 30
351 °C, where membrane fluidity and lipid packing order are decreased and compensating
352 levels of CL molecules are high, TamB becomes "clogged" by phospholipids with more
353 saturated phospholipids, impeding transport (**Fig. 6B**). Bulky and intrinsically disordered
354 CL molecules could contribute to the clogging sterically by obstructing the lipid channel
355 and precluding it from translocating other lipid substrates (i.e., PE). . Impaired transport
356 explains the difference in OM PE saturation profiles between the Δ*yhdP* Δ*fadR* strain and
357 the other, non-cold-sensitive strains. When Δ*tamB* is deleted, phospholipid flow is shifted
358 to YdbH, bypassing clogging and relieving cold sensitivity (**Fig. 6C**). YdbH's ability to
359 successfully transport phospholipids in the Δ*yhdP* Δ*tamB* strain only when TamB is absent
360 may be because YhdP and TamB are primary transporters (e.g., preferred interaction
361 partners for other pathway members), due to direct toxicity caused by TamB clogging, or
362 because *ydbH* is upregulated.

363 Several pieces of evidence demonstrate dysregulation of phospholipid transport not just
364 changes to OM phospholipid composition, and so permeability or physical strength, cause
365 the cold sensitivity phenotype of the Δ*yhdP* Δ*fadR* strain. First, the cold sensitivity is
366 unaffected by removing enterobacterial common antigen, which suppresses the
367 membrane permeability of a Δ*yhdP* strain (**Fig. 1C**, (40)), and the OM permeability
368 phenotypes of the Δ*yhdP* Δ*fadR* are not severe (**Fig. S2**). Second, the cold sensitivity is
369 suppressed by deletion of Δ*tamB* (**Fig. 1FG**). Δ*yhdP* Δ*tamB* strains have much greater OM
370 permeability (29) than the Δ*yhdP* or Δ*yhdP* Δ*fadR* strains. Third, CL has been shown to
371 have a normalizing, bidirectional, and leaflet-specific effect on lipid packing order (67, 68)
372 and membrane fluidity (69-72) opposite of or similar to that of cholesterol, respectively,
373 and so is unlike to contribute to a phenotype dependent solely on OM membrane fluidity.
374 Thus, the cold sensitivity phenotype correlates with the impairment of phospholipid
375 trafficking and the likely imbalance of phospholipids between the IM and OM and not
376 with the permeability phenotypes of the OM.

377 Although both fatty acid saturation and high CL levels are required for the Δ*yhdP* Δ*fadR*
378 strain's cold sensitivity, two lines of evidence point to saturation rather than headgroup
379 as the main factor separating YhdP and TamB function. (i) YhdP loss slows phospholipid
380 transport from the IM to the OM in a *mlaA** mutant, which losses OM material due to
381 vesiculation and lysis when phospholipid biosynthesis is insufficient to replace lost
382 phospholipids (24, 26). CL only accounts for 5% of phospholipids in exponentially growing

383 cells making unlikely loss of CL transport could slow net phospholipid transport to the
384 extent required to slow lysis. (ii) Δ*tamB* has a small growth defect at 30 °C (**Fig. 1G**) not
385 observed at higher temperature (29, 30), perhaps due to increased unsaturated
386 phospholipids (73-75) resulting in decreased net OM transport by YhdP or to lower OM
387 fluidity. Together, these observations provide strong evidence YhdP has a substrate
388 preference for phospholipids with more saturated fatty acids, while TamB prefers
389 phospholipids with more unsaturated fatty acids.

390 Our model suggests the IM and OM saturation state could be independently regulated
391 based on YhdP and TamB activity or levels. IM saturation is regulated by altering the
392 composition of newly synthesized fatty acids, while OM saturation could be separately
393 regulated by allowing increased transport of more saturated or unsaturated
394 phospholipids as necessary. IM and OM acyl saturation has been studied in several strains
395 of *E. coli* and in *Yersinia pseudotuberculosis* (7, 19-21) and higher saturated fatty acid
396 levels were observed in the OM than in the IM, supporting discrimination of phospholipids
397 transport based on saturation. The IM needs to maintain an appropriate level of fluidity
398 to allow IM proteins to fold and diffuse, to allow diffusion of hydrophobic molecules, to
399 regulate cellular respiration, and to maintain membrane integrity (76, 77). However, the
400 OM is a permeability barrier, a load-bearing element that resists turgor pressure (1-6),
401 and has an outer leaflet consisting of LPS (2, 8). LPS has saturated acyl chains and is largely
402 immobile in *E. coli* (78) and a specific phospholipid saturation level may be necessary to
403 match or counterbalance LPS rigidity. OM phospholipids may also play a role in the
404 physical strength of the membrane. Interestingly, previous work has demonstrated that
405 the tensile strength of the OM is lessened in a *yhdP* mutant (24).

406 Possessing two different phospholipid transporters with different saturation state
407 preferences would allow the cell to adapt OM saturation to changing conditions including
408 temperature shifts, chemical insults, or changes synthesis of other OM components (e.g.,
409 LPS or OMPs). A recent study demonstrated in *Y. pseudotuberculosis* the difference in
410 saturation levels between the membranes is exaggerated at 37 °C compared to 8 °C (21).
411 Thus, conditions where IM and OM saturation are independently regulated exist and this
412 regulation is likely important for optimum fitness of the cells. Transcriptional regulation
413 of *yhdP* and *tamB* has not been thoroughly explored. It seems likely *yhdP* transcription is
414 quite complex with several promoters and transcriptional termination sites (79-81). *tamB*
415 is predicted to be in an operon with *tamA* (which codes for an OMP necessary for TamB
416 function) and *ytfP* (79, 82) and to have a σ^E-dependent promoter (83). The σ^E stress
417 response is activated by unfolded OMP accumulation, and downregulates the production
418 of OMPs and upregulates chaperones and folding machinery (68). It is intriguing to
419 speculate a change in OM phospholipid composition might aid in OMP folding due to
420 altered biophysical properties and/or lipoprotein diffusion.

421 The mechanism of phospholipid transfer between the IM and OM has been one of the
422 largest remaining questions in gram-negative envelope biogenesis and has remained an

423 area of intense investigation for decades. Furthermore, given the lack of knowledge of
424 this pathway, the role of phospholipid composition in the permeability barrier of the OM,
425 and so the intrinsic antibiotic resistance of gram-negative bacteria, remains unknown.
426 Recent work has begun to elucidate the intermembrane phospholipid transport pathway
427 by identifying YhdP, TamB, and YdbH as proteins capable of transporting phospholipids
428 between the membranes (24, 29, 30). Our work has now clarified that YhdP and TamB
429 may have separate roles in phospholipid transport that are differentiated by their
430 preference for phospholipid saturation states and possibly lipid headgroup. Homologs of
431 YhdP and TamB are found throughout *Enterobacterales* and more distantly related
432 members of the ASMA family are wide spread in gram-negative bacteria (84). In fact,
433 TamB has recently been shown to play a role in anterograde intermembrane phospholipid
434 transport in the diderm Firmicute *Veillonella parvula* (38). Structural predictions of YhdP
435 and TamB are strikingly similar between species (31, 32). Given this, it is quite likely similar
436 mechanisms of discrimination in intermembrane phospholipid transfer exist in other
437 species. The data we present here provide a framework for investigation of phospholipid
438 transport and mechanisms differentiating phospholipid transporter function in these
439 species.
440
441
442 **Materials and Methods**

443 **Bacterial strains and Growth Conditions. Table S3** lists the strains used in this study. Most
444 knockout strains were constructed with Keio collection alleles using P1vir transduction
445 (85, 86). New alleles were constructed through λ-red recombineering (87), using the
446 primers indicated in **Table S4**. The FLP recombinase-FRT system was used to remove
447 antibiotic resistance cassettes as has been described (87). *E. coli* cultures were grown in
448 LB Lennox media at 42°C, unless otherwise mentioned. Where noted, LB was
449 supplemented with vancomycin (Gold Biotechnology), bacitracin (Gold Biotechnology),
450 SDS (Thermo Fisher Scientific), EDTA (Thermo Fisher Scientific), oleic acid (Sigma Aldrich),
451 stearic acid (Sigma Aldrich), arabinose (Gold Biotechnology), or glucose (Thermo
452 Scientific). For plasmid maintenance, media was supplemented with 25 µg/mL kanamycin
453 (Gold Biotechnology), 10 or 20 µg/mL chloramphenicol (Gold Biotechnology), or 10 µg/mL
454 tetracycline (Gold Biotechnology) as appropriate.

455 **Plasmid construction.** The pJW15-P_{fabA}, and pJW15-P_{fabA}(-19G>A) reporter plasmids were
456 constructed by amplifying the region upstream of *fabA* from -432 bp to +27 bp relative to
457 the annotated transcriptional start site from wild-type MG1655 or Suppressor 1,
458 respectively, using the Overlap-pJW15-*fabA* FP and RP primers (**Table S4**). pJW15 was
459 amplified using primers Overlap-pJW15-*fabA* FP1 and RP1. The pJW15 plasmid was a kind
460 of gift from Dr. Tracy Raivio (Univeristy of Alberta) (88, 89). The resulting fragments were
461 assembled using HiFi Assembly master mix (New England Biolabs) as per the
462 manufacturer's instructions.

463 **Growth and Sensitivity Assays.** For EOPs assays, cultures were grown overnight, serially
464 diluted, and plated on the indicated media. For *pgsA* depletion, overnight cultures grown
465 in arabinose were washed and diluted 1:100 into fresh LB with 0.2% glucose or arabinose
466 as indicated and grown to OD_{600}=1 before diluting and plating on media with glucose or
467 arabinose respective, as above. EOPs were incubated at 30 °C unless otherwise indicated.
468 Growth curves were performed at the indicated temperature as has been described (40).
469 For CPRG assays (44), strains were streaked on LB plates supplemented with CPRG
470 (40µg/ml) and IPTG (100 µM) incubated overnight at 30°C.

471 **Suppressor isolation and sequencing.** Serially diluted cultures were spread on LB plates
472 and incubated overnight at a 30°C. Colonies that grew at 30°C were isolated and
473 rechecked for cold-resistance through EOP and growth curves. The suppressors were
474 subjected to whole-genome sequencing to identify potential suppressor mutations.
475 Genomic DNA was isolated from the parent and suppressors using a DNeasy Blood and
476 Tissue Kit (Qiagen) as per the manufacturer's instructions. Library preparation and
477 Illumina sequencing were performed by the Microbial Genome Sequencing Center (MiGS,
478 Pittsburgh, PA, USA). Briefly, Illumina libraries were prepared and the libraries were
479 sequenced with paired-end 151 bp reads on a NextSeq 2000 platform to a read depth of
480 at least 200 Mbp. To identify variants from the reference genome (GenBank: U00096.3),
481 reads were trimmed to remove adaptors and the *breseq* software (version 0.35.4) was
482 used to call variants (90). Identified mutations were confirmed with Sanger sequencing.
483 The consensus motif of the FabR binding site of *fabA* was determined using Multiple Em
484 for Motif Elicitation (MEME) tool in the MEME Suite based on the sequence of putative
485 FabR binding sites reported by Feng and Cronan (2011) (58, 91, 92). The ability of the
486 identified P_{fabA} mutation to suppress was confirmed by linking the mutant to *zcb*-
487 3059::Tn*10* (93) and transducing to a clean background.

488 **Lux reporter assays.** Overnight cultures of strains harboring the pJW15-P_{fabA} and pJW15-
489 P_{fabA}(-19G>A) plasmids were sub-cultured at (1:100) into 200 µl of fresh LB broth in a black
490 96-well plate. The plate was incubated in a BioTek Synergy H1 plate reader and the OD_{600}
491 and luminescence intensity were recorded every 2.5 min for 6 hours as described in
492 previously (89, 94). Each biological replicate was performed in technical triplicate.

493 **RNA-seq.** Overnight cultures grown at 42°C were subcultured 1:100 into fresh media and
494 incubated at 42 °C until an OD_{600} of 0.4. Then, the cultures were shifted to a 30 °C water
495 bath for 30 minutes. 500 µL of each culture was immediately fixed in the RNAprotect
496 Bacteria Reagent (Qiagen) as per the manufacturer's instructions. RNA was purified using
497 the RNeasy Kit (Qiagen) with on-column DNase digestion following the manufacturer's
498 protocol for gram-negative bacteria. Library preparation, Illumina sequencing, and
499 analysis of differentially expressed genes were performed by MiGS. Briefly, samples were
500 treated with RNase free DNase (Invitrogen) and library preparation was performed with
501 the Stranded Total RNA Prep Ligation with Ribo-Zero Plus Kit (Illumina). Libraries were
502 sequenced with 2x50 bp reads on a NextSeq2000 (Illumina). Demultiplexing, quality

503 control, and adapter trimming carried out using bcl-convert (Illumina, v3.9.3) and
504 bcl2fastq (Illumina). Read mapping and read quantification were performed with HISAT2
505 (95) and the featureCounts tool in Subreader (96), respectively. Descriptive statistics of
506 the RNA-seq read data can be found in **Table S1**. The raw RNA-seq data is available in the
507 Sequence Read Archive database (SRA) (https://www.ncbi.nlm.nih.gov/sra, BioProject ID
508 PRJNA965821; Reviewer Access).

509 Raw read counts were normalized using the Trimmed Mean of M values algorithm in
510 edgeR (97) and converted to counts per million. The Quasi-Linear F-Test function of edgeR
511 was used for differential expression analysis. Normalized read values and for all genes as
512 well as differential expression analysis statistics can be found in **Dataset S3**. KEGG
513 pathway analysis was conducted using the *"kegga"* function of limma (98). Expression of
514 genes differentially expressed (greater than 2-fold change and $p<0.05$) was subjected to
515 principle component analysis, and pathway and enrichment analysis using the EcoCyc
516 Omics Dashboard (98).

517 **Lipid extraction and TLC.** For thin layer chromatography (TLC) experiments, cultures were
518 grown in LB with 1 mCi/mL ^{32}P until OD_{600} of 0.6-0.8 at the indicated temperature. For
519 temperature downshift experiments, cells were grown at 42 ^{o}C until OD_{600} of 0.2 and then
520 transferred to 30 ^{o}C for 2 hours. For lipid extraction, cells were pelleted and resuspended
521 in 0.2 mL of 0.5 M NaCl in 0.1 N HCl. Lipids were extracted by first adding 0.6 mL of
522 chloroform:methanol (1:2) to create a single-phase solution. After vigorous vortexing for
523 30 minutes, 0.2 mL of 0.5 M NaCl in 0.1 N HCl was added to convert the single-phase
524 solution to a two-phase solution. After centrifugation at 20 000 x g for 5 minutes at room
525 temperature, the lower phase was recovered and used for TLC. Approximately 2,000 cpm
526 of phospholipid extract was subjected to TLC analysis using a HPTLC 60 plate (EMD,
527 Gibbstown, NJ)) developed with either solvent 1: chloroform/methanol/acetic acid
528 [60/25/10 (vol/vol/vol) in **Fig. 2A** or by solvent 2: chloroform/methanol/ammonia/water
529 [65/37.5/3/1] (vol/vol/vol/vol) in **Fig. S4**. Radiolabeled lipids were visualized and
530 quantified using a Phosphoimager Typhoon FLA 9500 (GE). Images were processed and
531 quantified using ImageQuant™ software for scanning and analysis. The phospholipid
532 content is expressed as molecular percentage of the total phospholipids (correcting for
533 the two phosphates per molecule of CL).

534 **Phospholipid composition analysis.** Whole cell lipid extracts were isolated as for TLC
535 temperature downshift experiments without radiolabelling. IMs were isolated and
536 extracts were prepared as has been previously described (67). Briefly, cells from
537 temperature downshifted cultures were lysed using a French press at 8,000 psi and whole
538 cells were pelleted by centrifugation at 30 000 x g for 20 minutes. Then, the supernatant
539 was centrifuged at 150 000 x g for 1 hour. The resulting pellet contained pure IM as
540 demonstrated by immunoblot analysis (**Fig. S6A**). Relative amounts of CL, PG, and PE were
541 determined in these lipid extracts using liquid chromatography coupled to electrospray
542 ionization mass spectrometry (LC/MS) in an API 4000 mass spectrometer (Sciex,

543 Framingham, MA, USA) using normal phase solvents as previously published (99).
544 Individual molecular species of CL, PG, and PE were expressed as a percentage within their
545 individual phospholipid by summing all the species and dividing by that sum for each
546 phospholipid. The identities of CL species were confirmed using tandem mass
547 spectrometry.
548
549
550 **Acknowledgments**
551
552 We thank members of the Mitchell Lab for productive discussions. We would like to thank
553 Professor Tracy Raivio (University of Alberta) for the kind gift of pJW15 plasmid. This work
554 was funded by the National Institute of Allergy and Infectious Disease under Award
555 Number R01-AI155915 (to A.M.M.), the National Institute of General Medical Sciences
556 under Award Number R01-GM121493 (to M.B.), and Texas A&M University start-up funds
557 (to A.M.M.).
558
559
560 **References**

561 1. Nikaido H. 2003. Molecular basis of bacterial outer membrane permeability
562 revisited. Microbiology and Molecular Biology Reviews 67:593-656.
563 2. Silhavy TJ, Kahne D, Walker S. 2010. The bacterial cell envelope. Cold Spring
564 Harbor Perspectives in Biology 2.
565 3. Henderson JC, Zimmerman SM, Crofts AA, Boll JM, Kuhns LG, Herrera CM, Trent
566 MS. 2016. The power of asymmetry: Architecture and assembly of the Gram-
567 negative outer membrane lipid bilayer. Annual Review of Microbiology 70:255-
568 278.
569 4. Berry J, Rajaure M, Pang T, Young R. 2012. The spanin complex is essential for
570 lambda lysis. J Bacteriol 194:5667-74.
571 5. Rojas ER, Billings G, Odermatt PD, Auer GK, Zhu L, Miguel A, Chang F, Weibel DB,
572 Theriot JA, Huang KC. 2018. The outer membrane is an essential load-bearing
573 element in Gram-negative bacteria. Nature 559:617-621.
574 6. Navarro Llorens JM, Tormo A, Martinez-Garcia E. 2010. Stationary phase in gram-
575 negative bacteria. FEMS Microbiol Rev 34:476-95.
576 7. Lugtenberg EJJ, Peters R. 1976. Distribution of lipids in cytoplasmic and outer
577 membranes of *Escherichia coli* K12. Biochimica et Biophysica Acta (BBA) - Lipids
578 and Lipid Metabolism 441:38-47.
579 8. Kamio Y, Nikaido H. 1976. Outer membrane of *Salmonella typhimurium*:
580 accessibility of phospholipid head groups to phospholipase c and cyanogen
581 bromide activated dextran in the external medium. Biochemistry 15:2561-70.
582 9. Bogdanov M, Pyrshev K, Yesylevskyy S, Ryabichko S, Boiko V, Ivanchenko P,
583 Kiyamova R, Guan Z, Ramseyer C, Dowhan W. 2020. Phospholipid distribution in

584 the cytoplasmic membrane of Gram-negative bacteria is highly asymmetric,
585 dynamic, and cell shape-dependent. Science Advances 6:eaaz6333.
586 10. Benn G, Mikheyeva IV, Inns PG, Forster JC, Ojkic N, Bortolini C, Ryadnov MG,
587 Kleanthous C, Silhavy TJ, Hoogenboom BW. 2021. Phase separation in the outer
588 membrane of *Escherichia coli*. Proceedings of the National Academy of Sciences
589 118:e2112237118.
590 11. Konovalova A, Silhavy TJ. 2015. Outer membrane lipoprotein biogenesis: Lol is
591 not the end. Philosophical Transactions of the Royal Society B: Biological
592 Sciences 370:20150030.
593 12. Konovalova A, Kahne DE, Silhavy TJ. 2017. Outer Membrane Biogenesis. Annu
594 Rev Microbiol 71:539-556.
595 13. Lundstedt E, Kahne D, Ruiz N. 2021. Assembly and maintenance of lipids at the
596 bacterial outer membrane. Chemical Reviews 121:5098-5123.
597 14. John E. Cronan J, Rock CO. 2008. Biosynthesis of membrane lipids. EcoSal Plus 3.
598 15. Jones NC, Osborn MJ. 1977. Translocation of phospholipids between the outer
599 and inner membranes of *Salmonella typhimurium*. Journal of Biological
600 Chemistry 252:7405-7412.
601 16. Donohue-Rolfe AM, Schaechter M. 1980. Translocation of phospholipids from
602 the inner to the outer membrane of *Escherichia coli*. Proceedings of the National
603 Academy of Sciences 77:1867-1871.
604 17. Raetz CR, Kantor GD, Nishijima M, Newman KF. 1979. Cardiolipin accumulation in
605 the inner and outer membranes of *Escherichia coli* mutants defective in
606 phosphatidylserine synthetase. J Bacteriol 139:544-51.
607 18. Langley KE, Hawrot E, Kennedy EP. 1982. Membrane assembly: movement of
608 phosphatidylserine between the cytoplasmic and outer membranes of
609 *Escherichia coli*. J Bacteriol 152:1033-41.
610 19. White DA, Lennarz WJ, Schnaitman CA. 1972. Distribution of lipids in the wall
611 and cytoplasmic membrane subfractions of the cell envelope of *Escherichia coli*.
612 Journal of Bacteriology 109:686-690.
613 20. Ishinaga M, Kanamoto R, Kito M. 1979. Distribution of phospholipid molecular
614 species in outer and cytoplasmic membranes of *Escherichia coli*. The Journal of
615 Biochemistry 86:161-165.
616 21. Davydova L, Bakholdina S, Barkina M, Velansky P, Bogdanov M, Sanina N. 2016.
617 Effects of elevated growth temperature and heat shock on the lipid composition
618 of the inner and outer membranes of *Yersinia pseudotuberculosis*. Biochimie
619 123:103-109.
620 22. Osborn MJ, Gander JE, Parisi E, Carson J. 1972. Mechanism of Assembly of the
621 Outer Membrane of *Salmonella* typhimurium : Isolation and characterization of
622 cytoplasmic and outer membrane. Journal of Biological Chemistry 247:3962-
623 3972.
624 23. Bogdanov M. 2023. Renovating a double fence with or without notifying the next
625 door and across the street neighbors: why the biogenic cytoplasmic membrane

626 of Gram-negative bacteria display asymmetry? . Emerging Topics in Life Sciences
627 7:137-150.
628 24. Grimm J, Shi H, Wang W, Mitchell AM, Wingreen NS, Huang KC, Silhavy TJ. 2020.
629 The inner membrane protein YhdP modulates the rate of anterograde
630 phospholipid flow in *Escherichia coli*. Proc Natl Acad Sci U S A 117:26907-26914.
631 25. Malinverni JC, Silhavy TJ. 2009. An ABC transport system that maintains lipid
632 asymmetry in the Gram-negative outer membrane. Proceedings of the National
633 Academy of Sciences 106:8009-8014.
634 26. Sutterlin HA, Shi H, May KL, Miguel A, Khare S, Huang KC, Silhavy TJ. 2016.
635 Disruption of lipid homeostasis in the Gram-negative cell envelope activates a
636 novel cell death pathway. Proceedings of the National Academy of Sciences
637 113:E1565-E1574.
638 27. May KL, Silhavy TJ. 2018. The *Escherichia coli* phospholipase PldA regulates outer
639 membrane homeostasis via lipid signaling. mBio 9:e00379-18.
640 28. Tang X, Chang S, Qiao W, Luo Q, Chen Y, Jia Z, Coleman J, Zhang K, Wang T,
641 Zhang Z, Zhang C, Zhu X, Wei X, Dong C, Zhang X, Dong H. 2021. Structural
642 insights into outer membrane asymmetry maintenance in Gram-negative
643 bacteria by MlaFEDB. Nat Struct Mol Biol 28:81-91.
644 29. Ruiz N, Davis RM, Kumar S. 2021. YhdP, TamB, and YdbH are redundant but
645 essential for growth and lipid homeostasis of the gram-negative outer
646 membrane. mBio 12:e02714-21.
647 30. Douglass MV, McLean AB, Trent MS. 2022. Absence of YhdP, TamB, and YdbH
648 leads to defects in glycerophospholipid transport and cell morphology in Gram-
649 negative bacteria. PLOS Genetics 18:e1010096.
650 31. Jumper J, Evans R, Pritzel A, Green T, Figurnov M, Ronneberger O,
651 Tunyasuvunakool K, Bates R, Žídek A, Potapenko A, Bridgland A, Meyer C, Kohl
652 SAA, Ballard AJ, Cowie A, Romera-Paredes B, Nikolov S, Jain R, Adler J, Back T,
653 Petersen S, Reiman D, Clancy E, Zielinski M, Steinegger M, Pacholska M,
654 Berghammer T, Bodenstein S, Silver D, Vinyals O, Senior AW, Kavukcuoglu K,
655 Kohli P, Hassabis D. 2021. Highly accurate protein structure prediction with
656 AlphaFold. Nature 596:583-589.
657 32. Varadi M, Anyango S, Deshpande M, Nair S, Natassia C, Yordanova G, Yuan D,
658 Stroe O, Wood G, Laydon A, Žídek A, Green T, Tunyasuvunakool K, Petersen S,
659 Jumper J, Clancy E, Green R, Vora A, Lutfi M, Figurnov M, Cowie A, Hobbs N,
660 Kohli P, Kleywegt G, Birney E, Hassabis D, Velankar S. 2021. AlphaFold Protein
661 Structure Database: massively expanding the structural coverage of protein-
662 sequence space with high-accuracy models. Nucleic Acids Research 50:D439-
663 D444.
664 33. Josts I, Stubenrauch CJ, Vadlamani G, Mosbahi K, Walker D, Lithgow T, Grinter R.
665 2017. The structure of a conserved domain of TamB reveals a hydrophobic β taco
666 fold. Structure 25:1898-1906.e5.

667 34. Kumar N, Leonzino M, Hancock-Cerutti W, Horenkamp FA, Li P, Lees JA, Wheeler
668 H, Reinisch KM, De Camilli P. 2018. VPS13A and VPS13C are lipid transport
669 proteins differentially localized at ER contact sites. Journal of Cell Biology
670 217:3625-3639.
671 35. Valverde DP, Yu S, Boggavarapu V, Kumar N, Lees JA, Walz T, Reinisch KM, Melia
672 TJ. 2019. ATG2 transports lipids to promote autophagosome biogenesis. J Cell
673 Biol 218:1787-1798.
674 36. Otomo T, Maeda S. 2019. ATG2A transfers lipids between membranes *in vitro*.
675 Autophagy 15:2031-2032.
676 37. Osawa T, Kotani T, Kawaoka T, Hirata E, Suzuki K, Nakatogawa H, Ohsumi Y, Noda
677 NN. 2019. Atg2 mediates direct lipid transfer between membranes for
678 autophagosome formation. Nat Struct Mol Biol 26:281-288.
679 38. Grasekamp KP, Beaud B, Taib N, Audrain B, Bardiaux B, Rossez Y, Izadi-Pruneyre
680 N, Lejeune M, Trivelli X, Chouit Z, Guerardel Y, Ghigo J-M, Gribaldo S, Beloin C.
681 2023. Bridges instead of boats? The Mla system of diderm Firmicute *Veillonella*
682 *parvula* reveals an ancestral transenvelope core of phospholipid trafficking.
683 bioRxiv doi:10.1101/2023.06.30.547184:2023.06.30.547184.
684 39. Mitchell AM, Wang W, Silhavy TJ. 2017. Novel Rpos-dependent mechanisms
685 strengthen the envelope permeability barrier during stationary phase. J Bacteriol
686 199:e00708-16.
687 40. Mitchell AM, Srikumar T, Silhavy TJ. 2018. Cyclic enterobacterial common
688 antigen maintains the outer membrane permeability barrier of *Escherichia coli* in
689 a manner controlled by Yhdp. mBio 9:e01321-18.
690 41. Cronan JE. 2021. The *Escherichia coli* FadR transcription factor: Too much of a
691 good thing? Molecular Microbiology 115:1080-1085.
692 42. Nunn WD, Giffin K, Clark D, Cronan JE. 1983. Role for *fadR* in unsaturated fatty
693 acid biosynthesis in *Escherichia coli*. Journal of Bacteriology 154:554-560.
694 43. Rai AK, Mitchell AM. 2020. Enterobacterial common antigen: Synthesis and
695 function of an enigmatic molecule. mBio 11:e01914-20.
696 44. Paradis-Bleau C, Kritikos G, Orlova K, Typas A, Bernhardt TG. 2014. A genome-
697 wide screen for bacterial envelope biogenesis mutants identifies a novel factor
698 involved in cell wall precursor metabolism. PLoS Genet 10:e1004056.
699 45. Ruiz N, Falcone B, Kahne D, Silhavy TJ. 2005. Chemical conditionality: a genetic
700 strategy to probe organelle assembly. Cell 121:307-17.
701 46. Nikaido H, Vaara M. 1985. Molecular basis of bacterial outer membrane
702 permeability. Microbiol Rev 49:1-32.
703 47. Bishop RE. 2008. Structural biology of membrane-intrinsic β-barrel enzymes:
704 Sentinels of the bacterial outer membrane. Biochimica et Biophysica Acta (BBA) -
705 Biomembranes 1778:1881-1896.
706 48. Rowlett VW, Mallampalli V, Karlstaedt A, Dowhan W, Taegtmeyer H, Margolin W,
707 Vitrac H. 2017. Impact of membrane phospholipid slterations in *Escherichia coli*
708 on cellular function and bacterial stress adaptation. J Bacteriol 199.

709 49. Tan BK, Bogdanov M, Zhao J, Dowhan W, Raetz CRH, Guan Z. 2012. Discovery of
710 a cardiolipin synthase utilizing phosphatidylethanolamine and
711 phosphatidylglycerol as substrates. Proceedings of the National Academy of
712 Sciences 109:16504-16509.
713 50. Pluschke G, Hirota Y, Overath P. 1978. Function of phospholipids in *Escherichia*
714 *coli*. Characterization of a mutant deficient in cardiolipin synthesis. Journal of
715 Biological Chemistry 253:5048-5055.
716 51. Nishijima S, Asami Y, Uetake N, Yamagoe S, Ohta A, Shibuya I. 1988. Disruption of
717 the *Escherichia coli cls* gene responsible for cardiolipin synthesis. Journal of
718 Bacteriology 170:775-780.
719 52. Guo D, Tropp BE. 2000. A second *Escherichia coli* protein with CL synthase
720 activity. Biochimica et Biophysica Acta (BBA) - Molecular and Cell Biology of
721 Lipids 1483:263-274.
722 53. Kikuchi S, Shibuya I, Matsumoto K. 2000. Viability of an *Escherichia coli pgsA* null
723 mutant lacking detectable phosphatidylglycerol and cardiolipin. Journal of
724 Bacteriology 182:371-376.
725 54. Suzuki M, Hara H, Matsumoto K. 2002. Envelope disorder of *Escherichia coli* cells
726 lacking phosphatidylglycerol. Journal of Bacteriology 184:5418-5425.
727 55. Shiba Y, Yokoyama Y, Aono Y, Kiuchi T, Kusaka J, Matsumoto K, Hara H. 2004.
728 Activation of the Rcs signal transduction system is responsible for the
729 thermosensitive growth defect of an *Escherichia coli* mutant lacking
730 phosphatidylglycerol and cardiolipin. J Bacteriol 186:6526-35.
731 56. Grabowicz M, Silhavy TJ. 2017. Redefining the essential trafficking pathway for
732 outer membrane lipoproteins. Proceedings of the National Academy of Sciences
733 114:4769-4774.
734 57. Cronan JE, Jr., Gelmann EP. 1973. An estimate of the minimum amount of
735 unsaturated fatty acid required for growth of *Escherichia coli*. J Biol Chem
736 248:1188-95.
737 58. Feng Y, Cronan JE. 2011. Complex binding of the FabR repressor of bacterial
738 unsaturated fatty acid biosynthesis to its cognate promoters. Molecular
739 Microbiology 80:195-218.
740 59. Feng Y, Cronan JE. 2009. *Escherichia coli* unsaturated fatty acid synthesis:
741 Complex transcription of the *fabA* gene and *in vivo* identification of the essential
742 reaction catalyzed by FabB. Journal of Biological Chemistry 284:29526-29535.
743 60. Henry MF, Cronan JE. 1991. *Escherichia coli* transcription factor that both
744 activates fatty acid synthesis and represses fatty acid degradation. Journal of
745 Molecular Biology 222:843-849.
746 61. Henry MF, Cronan JE. 1992. A new mechanism of transcriptional regulation:
747 Release of an activator triggered by small molecule binding. Cell 70:671-679.
748 62. Rock CO, Jackowski S. 1985. Pathways for the incorporation of exogenous fatty
749 acids into phosphatidylethanolamine in *Escherichia coli*. J Biol Chem 260:12720-
750 4.

751 63. Français M, Bott R, Dargaignaratz C, Giniès C, Carlin F, Broussolle V, Nguyen-Thé
752 C. 2021. Short-Chain and Unsaturated Fatty Acids Increase Sequentially From the
753 Lag Phase During Cold Growth of *Bacillus cereus*. Frontiers in Microbiology 12.
754 64. Heath RJ, Rock CO. 1996. Roles of the FabA and FabZ β-hydroxyacyl-acyl carrier
755 protein dehydratases in *Escherichia coli* fatty acid biosynthesis. Journal of
756 Biological Chemistry 271:27795-27801.
757 65. Ostrander DB, Sparagna GC, Amoscato AA, McMillin JB, Dowhan W. 2001.
758 Decreased Cardiolipin Synthesis Corresponds with Cytochromec Release in
759 Palmitate-induced Cardiomyocyte Apoptosis. Journal of Biological Chemistry
760 276:38061-38067.
761 66. Lewis RNAH, Zweytick D, Pabst G, Lohner K, McElhaney RN. 2007. Calorimetric,
762 X-Ray Diffraction, and Spectroscopic Studies of the Thermotropic Phase Behavior
763 and Organization of Tetramyristoyl Cardiolipin Membranes. Biophysical Journal
764 92:3166-3177.
765 67. Bogdanov M, Sun J, Kaback HR, Dowhan W. 1996. A Phospholipid Acts as a
766 Chaperone in Assembly of a Membrane Transport Protein. Journal of Biological
767 Chemistry 271:11615-11618.
768 68. Mitchell AM, Silhavy TJ. 2019. Envelope stress responses: balancing damage
769 repair and toxicity. Nature Reviews Microbiology 17:417-428.
770 69. Shibata A, Ikawa K, Shimooka T, Terada H. 1994. Significant stabilization of the
771 phosphatidylcholine bilayer structure by incorporation of small amounts of
772 cardiolipin. Biochimica et Biophysica Acta (BBA) - Biomembranes 1192:71-78.
773 70. Boscia AL, Treece BW, Mohammadyani D, Klein-Seetharaman J, Braun AR,
774 Wassenaar TA, Klösgen B, Tristram-Nagle S. 2014. X-ray structure,
775 thermodynamics, elastic properties and MD simulations of
776 cardiolipin/dimyristoylphosphatidylcholine mixed membranes. Chemistry and
777 Physics of Lipids 178:1-10.
778 71. Pennington ER, Fix A, Sullivan EM, Brown DA, Kennedy A, Shaikh SR. 2017.
779 Distinct membrane properties are differentially influenced by cardiolipin content
780 and acyl chain composition in biomimetic membranes. Biochimica et Biophysica
781 Acta (BBA) - Biomembranes 1859:257-267.
782 72. Lopes SC, Ivanova G, de Castro B, Gameiro P. 2018. Revealing cardiolipins
783 influence in the construction of a significant mitochondrial membrane model.
784 Biochimica et Biophysica Acta (BBA) - Biomembranes 1860:2465-2477.
785 73. Marr AG, Ingraham JL. 1962. Effect of temperature on the composition of fatty
786 acids in *Escherichia coli*. Journal of Bacteriology 84:1260-1267.
787 74. Garwin JL, Klages AL, Cronan JE. 1980. Beta-ketoacyl-acyl carrier protein
788 synthase II of *Escherichia coli*. Evidence for function in the thermal regulation of
789 fatty acid synthesis. Journal of Biological Chemistry 255:3263-3265.
790 75. de Mendoza D, Klages Ulrich A, Cronan JE. 1983. Thermal regulation of
791 membrane fluidity in *Escherichia coli*. Effects of overproduction of beta-ketoacyl-
792 acyl carrier protein synthase I. Journal of Biological Chemistry 258:2098-2101.

793 76. Knapp BD, Huang KC. 2022. The effects of temperature on cellular physiology.
794 Annual Review of Biophysics 51:499-526.
795 77. Bogdanov M, Umeda M, Dowhan W. 1999. Phospholipid-assisted refolding of an
796 integral membrane protein: Minimum structural features for
797 phosphatidylethanolamine to act as a molecular chaperone. Journal of Biological
798 Chemistry 274:12339-12345.
799 78. Raetz CR, Whitfield C. 2002. Lipopolysaccharide endotoxins. Annu Rev Biochem
800 71:635-700.
801 79. Conway T, Creecy JP, Maddox SM, Grissom JE, Conkle TL, Shadid TM, Teramoto J,
802 Miguel PS, Shimada T, Ishihama A, Mori H, Wanner BL. 2014. Unprecedented
803 high-resolution view of bacterial operon architecture revealed by RNA
804 sequencing. mBio 5:e01442-14.
805 80. Thomason MK, Bischler T, Eisenbart SK, Förstner KU, Zhang A, Herbig A, Nieselt
806 K, Sharma CM, Storz G. 2015. Global transcriptional start site mapping using
807 differential RNA sequencing reveals novel antisense rnas in *Escherichia coli*.
808 Journal of Bacteriology 197:18-28.
809 81. Adams PP, Baniulyte G, Esnault C, Chegireddy K, Singh N, Monge M, Dale RK,
810 Storz G, Wade JT. 2021. Regulatory roles of *Escherichia coli* 5' UTR and ORF-
811 internal RNAs detected by 3' end mapping. eLife 10:e62438.
812 82. Karp PD, Ong WK, Paley S, Billington R, Caspi R, Fulcher C, Kothari A,
813 Krummenacker M, Latendresse M, Midford PE, Subhraveti P, Gama-Castro S,
814 Muñiz-Rascado L, Bonavides-Martinez C, Santos-Zavaleta A, Mackie A, Collado-
815 Vides J, Keseler IM, Paulsen I. 2018. The EcoCyc database. EcoSal Plus
816 8:10.1128/ecosalplus.ESP-0006-2018.
817 83. Huerta AM, Collado-Vides J. 2003. Sigma70 promoters in *Escherichia coli*: specific
818 transcription in dense regions of overlapping promoter-like signals. Journal of
819 Molecular Biology 333:261-278.
820 84. Szklarczyk D, Gable AL, Nastou KC, Lyon D, Kirsch R, Pyysalo S, Doncheva NT,
821 Legeay M, Fang T, Bork P, Jensen LJ, von Mering C. 2021. The STRING database in
822 2021: customizable protein-protein networks, and functional characterization of
823 user-uploaded gene/measurement sets. Nucleic Acids Res 49:D605-d612.
824 85. Baba T, Ara T, Hasegawa M, Takai Y, Okumura Y, Baba M, Datsenko KA, Tomita
825 M, Wanner BL, Mori H. 2006. Construction of *Escherichia coli* K-12 in-frame,
826 single-gene knockout mutants: the Keio collection. Mol Syst Biol 2:2006.0008-
827 2006.0008.
828 86. Silhavy TJ, Berman ML, Enquist LW. 1984. Experiments with gene fusions. Cold
829 Spring Harbor Laboratory.
830 87. Datsenko KA, Wanner BL. 2000. One-step inactivation of chromosomal genes in
831 *Escherichia coli* K-12 using PCR products. Proceedings of the National Academy
832 of Sciences 97:6640-6645.
833 88. MacRitchie DM, Ward JD, Nevesinjac AZ, Raivio TL. 2008. Activation of the Cpx
834 envelope stress response down-regulates expression of several locus of

835 enterocyte effacement-encoded genes in enteropathogenic *Escherichia coli*.
836 Infection and Immunity 76:1465-1475.
837 89. Wong JL, Vogt SL, Raivio TL. 2013. Using reporter genes and the *Escherichia coli*
838 ASKA overexpression library in screens for regulators of the Gram negative
839 envelope stress response. Methods Mol Biol 966:337-57.
840 90. Deatherage DE, Barrick JE. 2014. Identification of mutations in laboratory-
841 evolved microbes from next-generation sequencing data using breseq. Methods
842 Mol Biol 1151:165-88.
843 91. Bailey TL, Elkan C. 1994. Fitting a mixture model by expectation maximization to
844 discover motifs in biopolymers. Proc Int Conf Intell Syst Mol Biol 2:28-36.
845 92. Bailey TL, Johnson J, Grant CE, Noble WS. 2015. The MEME Suite. Nucleic Acids
846 Res 43:W39-49.
847 93. Singer M, Baker TA, Schnitzler G, Deischel SM, Goel M, Dove W, Jaacks KJ,
848 Grossman AD, Erickson JW, Gross CA. 1989. A collection of strains containing
849 genetically linked alternating antibiotic resistance elements for genetic mapping
850 of Escherichia coli. Microbiol Rev 53:1-24.
851 94. Rai AK, Carr JF, Bautista DE, Wang W, Mitchell AM. 2021. ElyC and cyclic
852 enterobacterial common antigen regulate synthesis of phosphoglyceride-linked
853 enterobacterial common antigen. mBio 12:e02846-21.
854 95. Kim D, Paggi JM, Park C, Bennett C, Salzberg SL. 2019. Graph-based genome
855 alignment and genotyping with HISAT2 and HISAT-genotype. Nature
856 Biotechnology 37:907-915.
857 96. Liao Y, Smyth GK, Shi W. 2013. featureCounts: an efficient general purpose
858 program for assigning sequence reads to genomic features. Bioinformatics
859 30:923-930.
860 97. Robinson MD, McCarthy DJ, Smyth GK. 2009. edgeR: a Bioconductor package for
861 differential expression analysis of digital gene expression data. Bioinformatics
862 26:139-140.
863 98. Ritchie ME, Phipson B, Wu D, Hu Y, Law CW, Shi W, Smyth GK. 2015. limma
864 powers differential expression analyses for RNA-sequencing and microarray
865 studies. Nucleic Acids Research 43:e47-e47.
866 99. Sparagna GC, Johnson CA, McCune SA, Moore RL, Murphy RC. 2005.
867 Quantitation of cardiolipin molecular species in spontaneously hypertensive
868 heart failure rats using electrospray ionization mass spectrometry. J Lipid Res
869 46:1196-204.

870
871

Figures and Tables

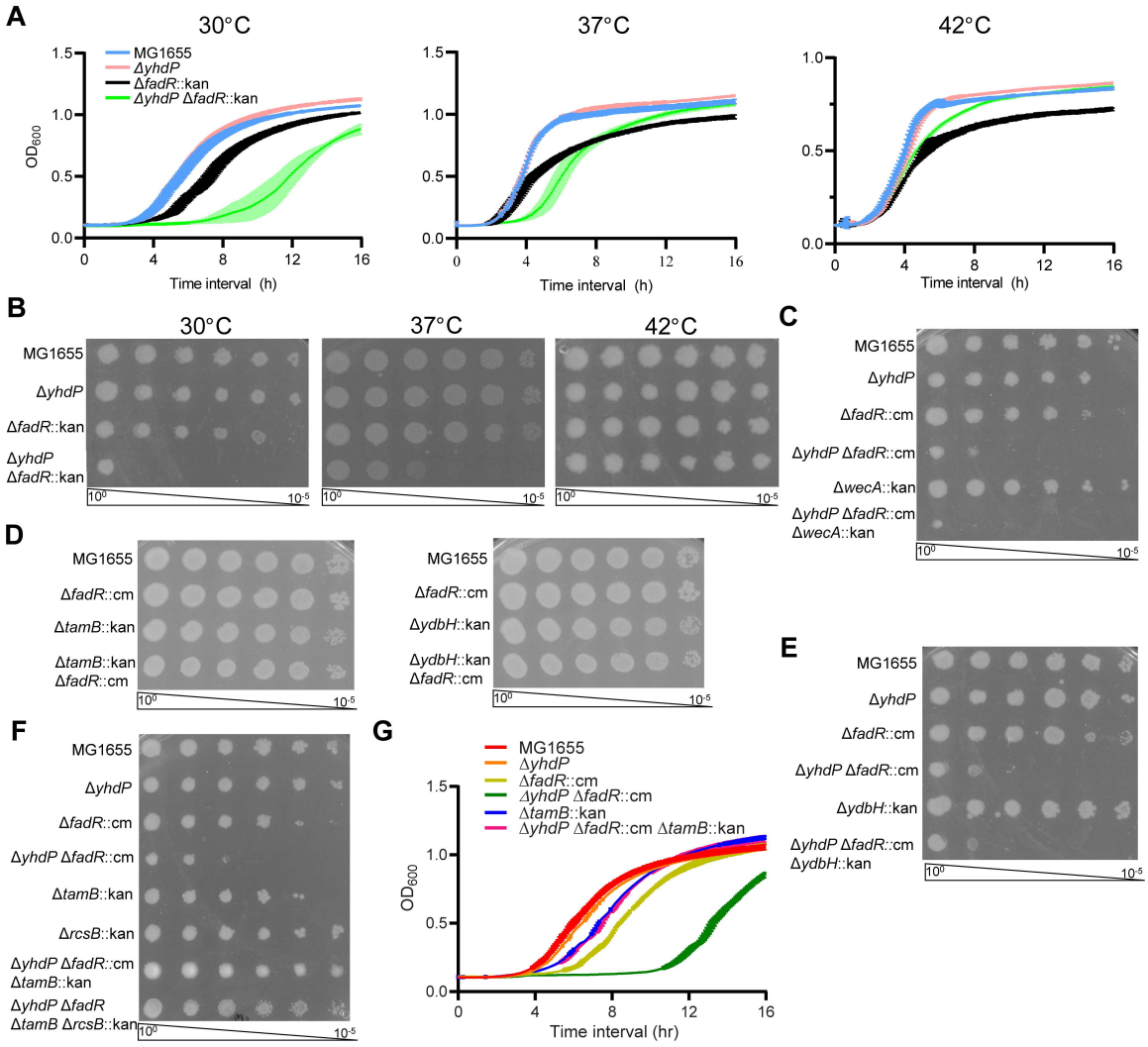

Figure 1. Deletion of *yhdP* and *fadR* causes synthetic cold sensitivity due to impairment of TamB function. (A) The Δ*yhdP* Δ*fadR* strain had impaired growth at lower temperatures. **(B)** EOPs were performed to confirm the growth defect of the Δ*yhdP* Δ*fadR* strain. **(C-F)** EOPs were performed at 30 °C to assess cold sensitivity. **(C)** The growth of the Δ*yhdP* Δ*fadR* strain was not affected by the loss of ECA (Δ*wecA*). **(D)** Neither a Δ*tamB* Δ*fadR* strain nor a Δ*ydbH* Δ*fadR* strain exhibited cold sensitivity. **(E)** Deletion of *ydbH* did not suppress cold sensitivity in the Δ*yhdP* Δ*fadR* strain. **(F)** Deletion of *tamB* completely suppressed cold sensitivity in the Δ*yhdP* Δ*fadR* strain and the Rcs stress response was not necessary for this suppression. **(G)** Growth curves were performed at 30 °C . The Δ*tamB* and the Δ*yhdP* Δ*fadR* Δ*tamB* strain grew equally well, indicating suppression is unlikely to result from slow growth. Quantitative data are shown as the mean of three biological replicates ± the SEM. Images are representative of three independent experiments.

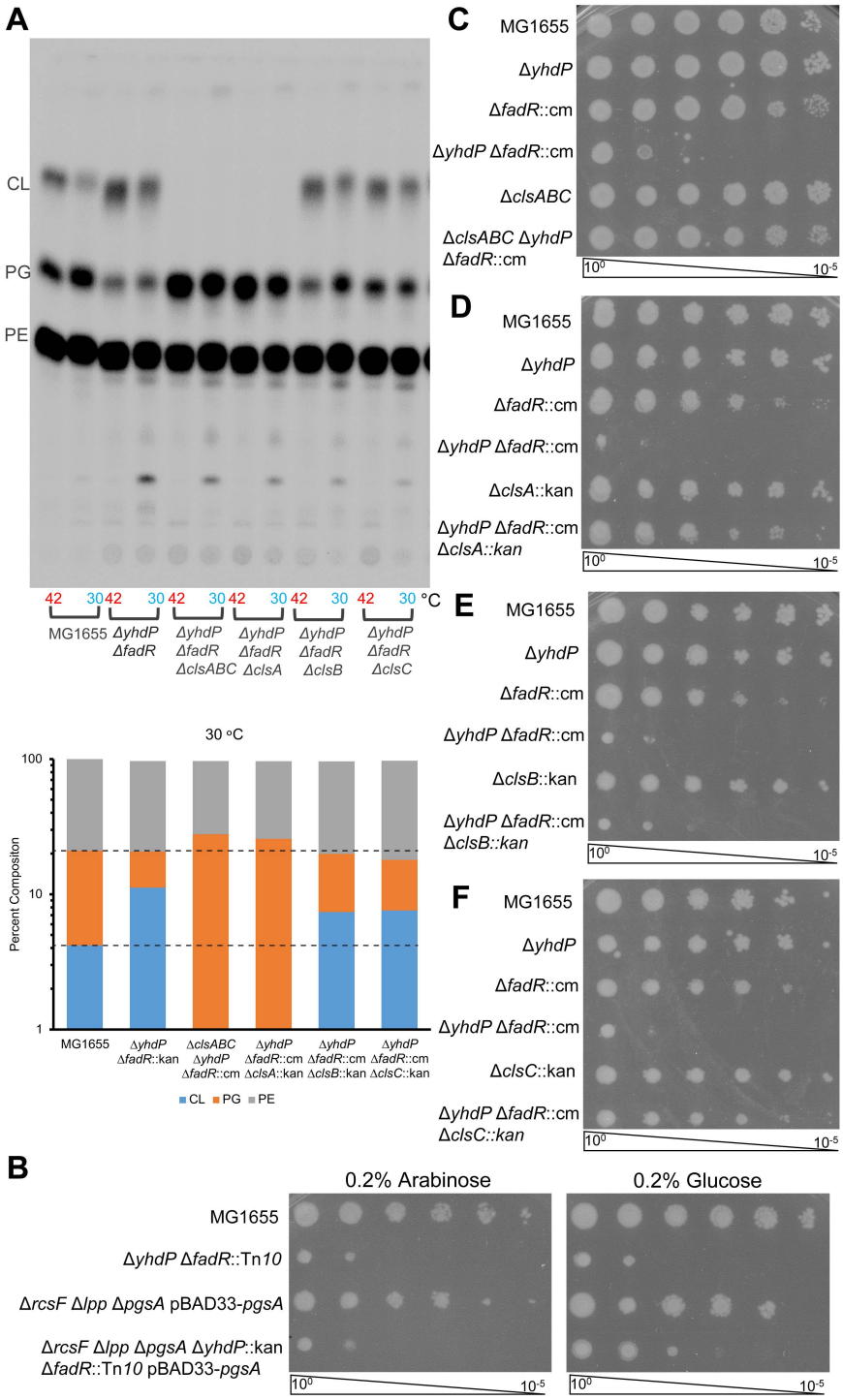

Figure 2. Increased cardiolipin levels are necessary for cold sensitivity of the Δ*yhdP* Δ*fadR* strain. (A) Thin layer chromatography (TLC) of lipid extracts was performed for the indicated cultures grown to OD_{600}=0.2 at 42 °C then transferred to 30 °C or 42 °C for 2 hours before analysis. Relative phospholipid levels are provided for 30 °C samples. The Δ*yhdP* Δ*fadR* strain shows increased levels of CL and a concomitant decrease in PG levels.

894 **(B-F)** Growth effects of altered phospholipid levels were investigated by EOP. Images are
895 representative of three independent experiments. **(B)** PgsA depletion strains in a
896 background where *pgsA* is non-essential were used to assay the effect of lowering PG and
897 CL levels on cold sensitivity. Arabinose induces expression of *pgsA* while glucose
898 represses. Lowering PG and CL levels partially suppressed cold sensitivity. **(C)** Deletion of
899 the three CL synthases, *clsA*, *clsB*, and *clsC*, suppressed cold sensitivity of the Δ*yhdP* Δ*fadR*
900 strain. **(D)** Deletion of *clsA* also suppressed cold sensitivity. **(E)** Deletion of *clsB* does not
901 suppress cold sensitivity, while deletion of *clsC* (F) does.
902
903

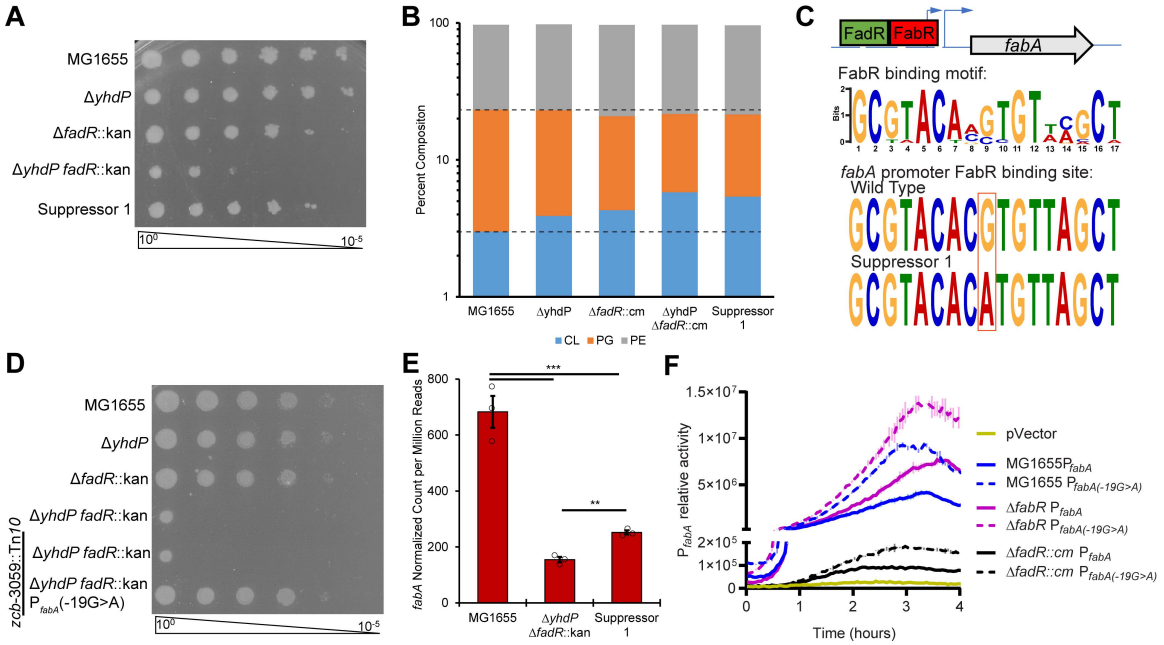

Figure 3. Cold sensitivity can be suppressed by increasing *fabA* expression. (A) The cold sensitivity of a spontaneous suppressor of Δ*yhdP* Δ*fadR* cold sensitivity was tested by EOP. The suppressor returned growth to the level of the Δ*fadR* mutant. **(B)** TLC was performed to assay phospholipid composition. Suppressor 1 showed very similar phospholipid composition to that of its parent strain and did not decrease CL levels. **(C)** A diagram of the promoter region of *fabA* is shown with its transcriptional start sites (blue arrows) and regulator binding sites (boxes). FadR acts as an activator while FabR acts as a repressor. The motif of the FabR binding site, generated using MEME, is shown with the sequences of the parent strain and of Suppressor 1. **(D)** The P_{fabA}(-19G>A) mutation was linked to a Tn*10* and transferred to the Δ*yhdP* Δ*fadR* strain by transduction. The Δ*yhdP* Δ*fadR* strain with P_{fabA}(-19G>A) was not cold sensitivity, confirming suppression. **(E)** *fabA* RNA levels are shown. Bars are the mean of three biological replicates ± the SEM. Individual data points are shown as open circles. ** $p<0.005$, *** $p<0.0005$ by quasi-linear F-test. Data are from the RNA-seq experiment in Figure 5 and *fabA* data are also shown in Figure 5F. **(F)** Luciferase reporters of wild-type and mutant *fabA* promoter activity were constructed. The mutation caused similar fold increases in P_{fabA} activity in all strain backgrounds. Data are luminescence relative to OD_{600} and are shown as the average of two biological replicates ± the SEM.

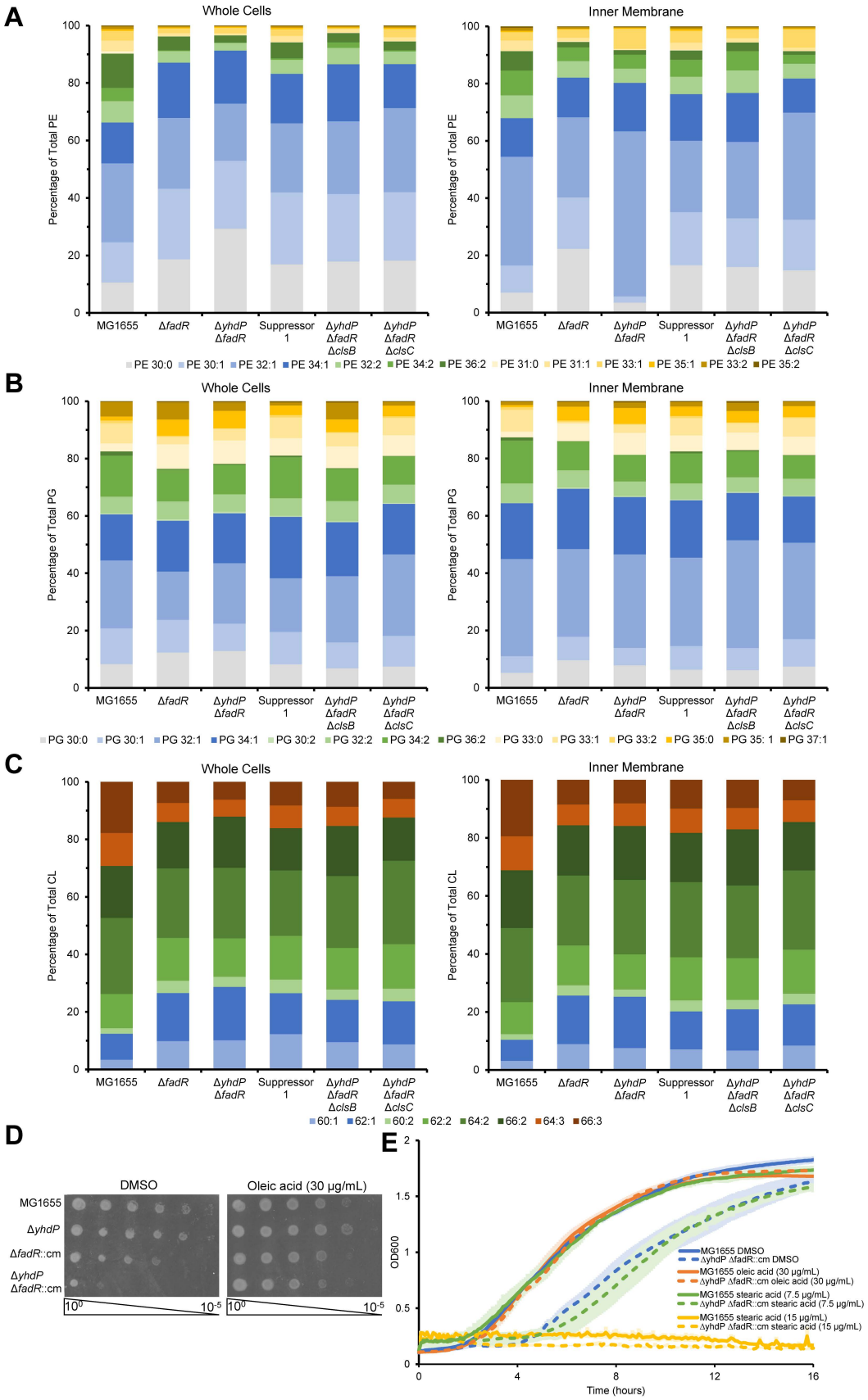
A
Whole Cells
Inner Membrane
Percentage of Total PE
MG1655
ΔfadR
ΔyhdP ΔfadR
Suppressor 1
ΔyhdP ΔfadR ΔclsB
ΔyhdP ΔfadR ΔclsC
PE 30:0 PE 30:1 PE 32:1 PE 34:1 PE 32:2 PE 34:2 PE 36:2 PE 31:0 PE 31:1 PE 33:1 PE 35:1 PE 33:2 PE 35:2
B
Whole Cells
Inner Membrane
Percentage of Total PG
PG 30:0 PG 30:1 PG 32:1 PG 34:1 PG 30:2 PG 32:2 PG 34:2 PG 36:2 PG 33:0 PG 33:1 PG 33:2 PG 35:0 PG 35: 1 PG 37:1
C
Whole Cells
Inner Membrane
Percentage of Total CL
60:1 62:1 60:2 62:2 64:2 66:2 64:3 66:3
D
DMSO
Oleic acid (30 µg/mL)
MG1655
ΔyhdP
ΔfadR::cm
ΔyhdP ΔfadR::cm
10^0
10^-5
E
OD600
Time (hours)
MG1655 DMSO
ΔyhdP ΔfadR::cm DMSO
MG1655 oleic acid (30 µg/mL)
ΔyhdP ΔfadR::cm oleic acid (30 µg/mL)
MG1655 stearic acid (7.5 µg/mL)
ΔyhdP ΔfadR::cm stearic acid (7.5 µg/mL)
MG1655 stearic acid (15 µg/mL)
ΔyhdP ΔfadR::cm stearic acid (15 µg/mL)

925 **Figure 4. Decreasing fatty acid saturation suppresses Δ*yhdP* Δ*fadR* cold sensitivity. (A-**
926 **C)** Lipid extracts were made from whole cells or from IM separated from OM by
927 differential centrifugation. Strains were grown to OD_{600} 0.2 at 42 °C then shifted to 30 °C
928 for 2 hours before harvest. Lipid extracts were quantified using LC/MS and the percentage
929 of each specific species of PE (A), PG (B), and CL (C) was calculated using the sum of all
930 molecular species detected. Suppressor 1 showed decreased saturation compared to its
931 parent strain (Δ*yhdP* Δ*fadR*). For PE, this difference was evident for whole cells but not
932 for IM. Data for phospholipids without unsaturations are shown in grey, with one
933 unsaturation in blue, with two unsaturations in green, with three unsaturations in orange,
934 and odd chain fatty acids (likely cyclopropyl-fatty acids) in yellow. Data for phospholipids
935 with longer acyl chains are shown in darker colors. **(D)** EOPS were performed on media
936 supplemented with oleic acid or a vehicle control. Oleic acid suppresses the cold
937 sensitivity of the Δ*yhdP* Δ*fadR* strain. **(E)** Growth curves of the indicated strains were
938 performed in the presence of oleic acid, stearic acid, or a vehicle control. Oleic acid
939 suppressed the cold sensitivity of the Δ*yhdP* Δ*fadR* strain while stearic acid did not. Data
940 are the average of three biological replicates ± the SEM.
941

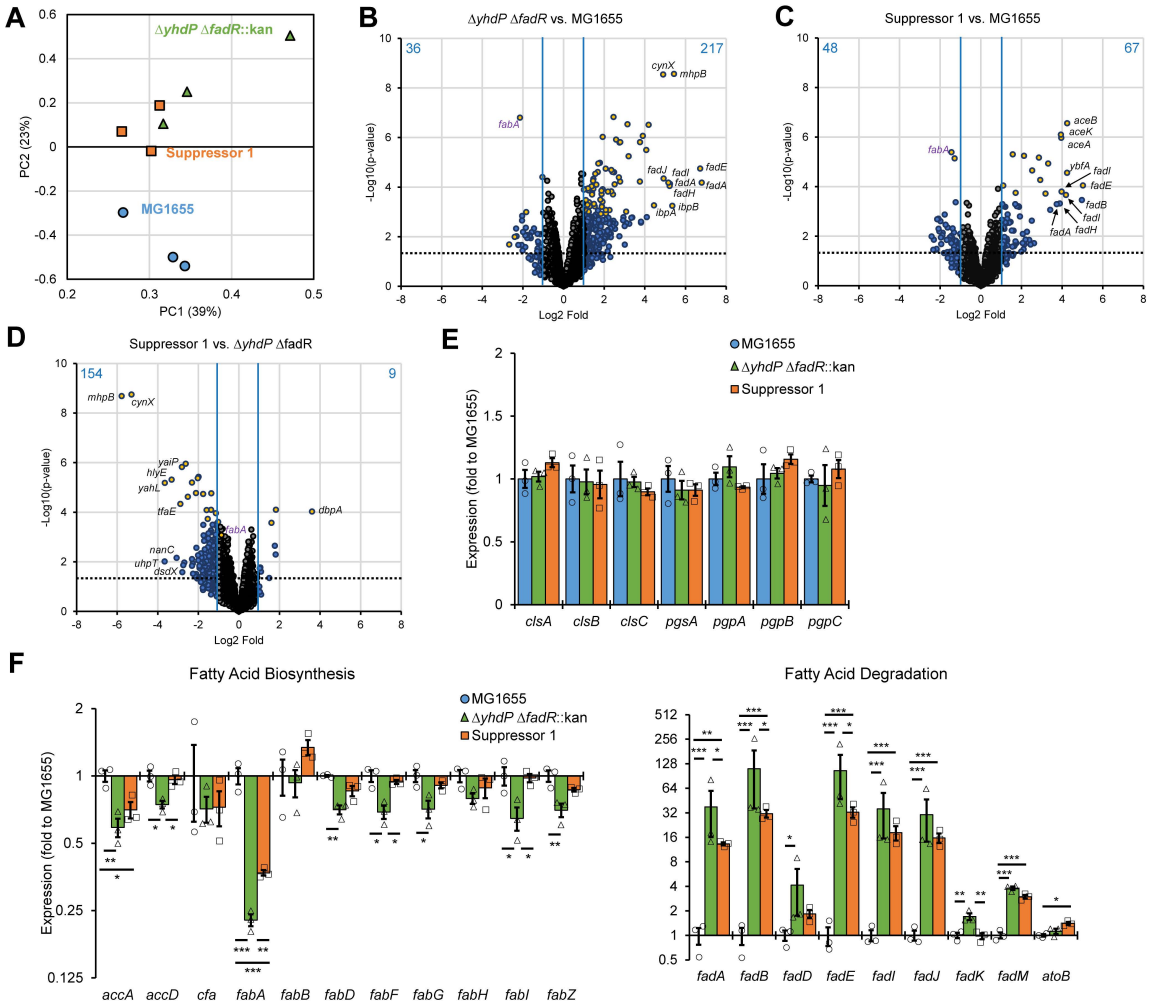

Figure 5. Transcriptional landscape of the Δ*yhdP* Δ*fadR* and suppressed strain. Three biological replicates of the indicated strains were grown at 42 °C to mid-log then transferred to 30 °C for 30 minutes before harvesting RNA and performing RNA-seq. Differential expression was calculated based on a greater than 2-fold change in expression and a p value of less than 0.05 by quasi-linear F-test. **(A)** PCA was performed on the expression of all genes differentially expressed between any groups of samples. Suppressor 1 and the Δ*yhdP* Δ*fadR* strain grouped closer together than to the wild-type strain, although Suppressor 1 was closer to wild type than the Δ*yhdP* Δ*fadR* strain. **(B-D)** Volcano plots show the average fold change and significance of expression changes between the Δ*yhdP* Δ*fadR* strain and wild-type MG1655 (B), Suppressor 1 and wild-type MG1655 (C), and Suppressor 1 and the Δ*yhdP* Δ*fadR* strain (D). Genes with changes greater than 2-fold are shown in blue, while genes with changes less than 2-fold are shown in grey. Genes with a q-value (false discovery rate) of less than 0.05 are shown in yellow. Blue lines indicate a 2-fold change and dotted line indicates p>0.05. The number of up or down regulated genes is indicated in blue. The names of the 10 genes with the largest changes are called out. More genes were up-regulated then down regulated in the Δ*yhdP* Δ*fadR* strain and Suppressor 1 vs. wild type. More genes were down regulated in

960 Suppressor 1 compared to the Δ*yhdP* Δ*fadR* strain. **(E)** Relative expression of genes in the
961 CL synthesis pathway is shown as averages ± the SEM and individual data points. No
962 significant changes were evident. **(F)** Relative expression of genes in the fatty acid
963 synthesis and degradation pathways is shown as averages ± the SEM and individual data
964 points. A general normalizing of these pathways occurred in Suppressor 1 compared to
965 the Δ*yhdP* Δ*fadR* strain; however, the most significant change was in the expression of
966 *fabA*. * $p<0.05$, ** $p<0.005$, *** $p<0.0005$ by quasi-linear F-test.
967

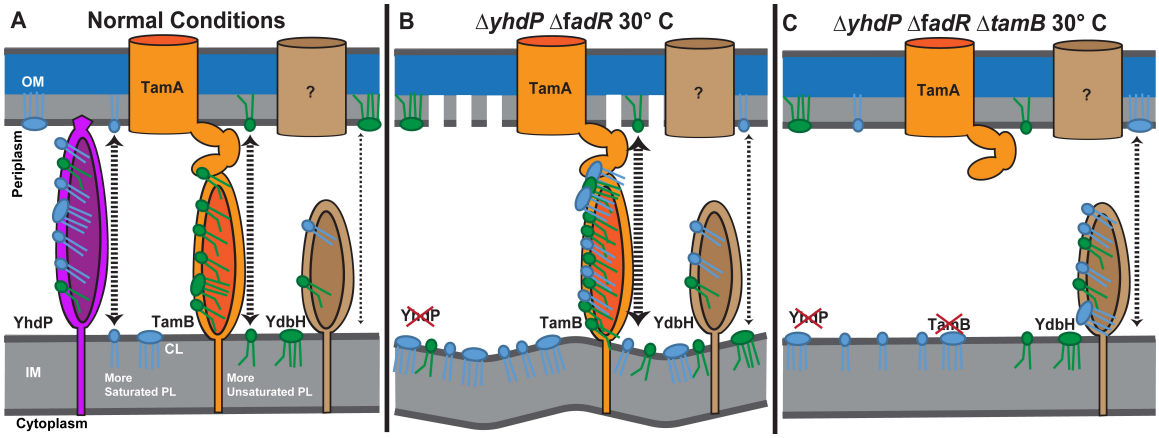

Figure 6. Model for the role of YhdP and TamB in phospholipid transport. Our data can be explained by the following model of phospholipid transport. **(A)** In normal conditions, YhdP is mainly responsible for the transport of phospholipids with more saturated fatty acid chains between the IM and OM. TamB shows a strong preference for transporting phospholipids with more unsaturated fatty acids, with YdbH playing a minor role in phospholipid transport. **(B)** In the Δ*yhdP* Δ*fadR* strain, YhdP is not available to transport more saturated phospholipids and the proportion of both saturated fatty acids and cardiolipin is increased, especially at low temperature. The fluidity of the membrane is also lessened by the low temperature. In these conditions, transport of phospholipids between the membranes is impeded, due to clogging of TamB by a combination of less saturated phospholipids and/or bulky and highly disordered CL. This leads to a lethal lack of phospholipids in the OM and overabundance of phospholipids in the IM. **(C)** When *tamB* is deleted in the Δ*yhdP* Δ*fadR* strain, the clogging of TamB is relieved, and the cell relies on YdbH for phospholipid transport overcoming the cold sensitivity. PL: phospholipid